

Symmetry-Based Analysis of the Effects of Random Energy Disorder on the Excitonic Level Structure of Cyclic Arrays: Application to Photosynthetic Antenna Complexes

H.-M. Wu and G. J. Small*

Ames Laboratory-USDOE and Department of Chemistry, Iowa State University, Ames, Iowa 50011

Received: September 10, 1997; In Final Form: November 13, 1997

We extend the work of Wu and Small who introduced symmetry-adapted basis defect patterns (BDPs) for systematic analysis of the effects of random static energy disorder (diagonal or off-diagonal) on the excitonic level structure of cyclic C_n arrays of chromophores. Examples include the B850 and B875 rings of bacteriochlorophyll (BChl) molecules associated with the LH2 and LH1 antenna complexes of purple bacteria for which, so far, $n = 8, 9$, and 16 . Calculation of the localization/extendedness (chromophore occupation number) patterns and participation numbers of the exciton levels reveals that the effects of random disorder on the exciton levels that contribute to the critically important B850 or B875 absorption band can be understood in terms of a single BDP of e_1 symmetry ("hidden correlation" effect). This is a consequence of the structures of the complexes, the complexes falling in the weak disorder regime and the strict symmetry selection rules that govern the couplings between zero-order exciton levels by BDPs. The above finding greatly simplifies computational studies on the effects of random disorder on the spectroscopic properties of the above bands. Our results show that interpretation of electric field (Stark) effects on the B850 and B875 absorption bands must include the effects of energy disorder. Similarities and differences between the effects of diagonal and off-diagonal energy disorder are discussed as is the relevance of our findings to the superradiant properties of the LH complexes.

1. Introduction

We recently introduced symmetry-adapted basis defect patterns (BDPs) for analysis of the effects of static diagonal and off-diagonal energy disorder on the excitonic structure and spectroscopic properties of cyclic (C_n) arrays of coupled chromophores.^{1,2} Motivation for doing so was that light-harvesting (LH) antenna complexes of purple photosynthetic bacteria exhibit C_n symmetry with $n = 8,^3 9,^4$ and $16,^5$ the chromophore being a bacteriochlorophyll (BChl) molecule. The LH2 complex of *Rhodospseudomonas acidophila* is an example of C_9 with nine α, β polypeptide pairs, each of which bind a pair of BChl molecules at the periplasmic side of the membrane. The 18 strongly coupled BChl molecules with nearest neighbor couplings of $\sim 300 \text{ cm}^{-1}$ ⁶ give rise to the B850 absorption band shown in Figure 1 for the isolated complex at 4.2 K.⁷ The structure of the BChl pair is such that essentially only its lowest energy excitonic component carries absorption intensity.⁸ It turns out that² the exciton levels which contribute to the B850 band are well described by the Hamiltonian indicated by the circular array of nine transition dipoles shown in Figure 1. Each dipole corresponds to that of the lowest energy component of the BChl pair. To a high degree of accuracy, these dipoles can be taken to be perpendicular to the C_9 rotation axis. Recent experimental data have led to a value of approximately -300 cm^{-1} for the nearest neighbor dimer-dimer dipole coupling (V) at cryogenic temperatures.⁹ The excitonic level structure from ref 9 calculated with $V = -320 \text{ cm}^{-1}$ and eq 3 of this paper is shown below the absorption spectrum in Figure 1. The relative energies of the levels are in the unit of cm^{-1} . Each level is labeled by its C_9 irreducible representation rep A or E_j with $j = 1-4$ (see section 2 for further discussion). Only the A level and separably degenerate E_1 level are symmetry allowed in

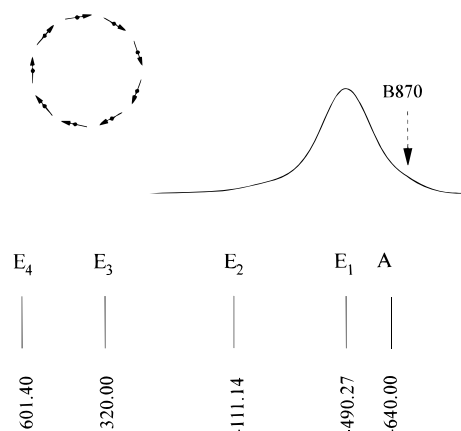


Figure 1. The 4.2 K absorption profile of B850 of the LH2 complex from *Rps. acidophila*. The dashed arrow indicates the low energy tail absorption due to the lowest A exciton level, B870. At the bottom is the exciton level structure in the absence of disorder calculated with eq 3 and a nearest dimer–dimer coupling of $V = -320 \text{ cm}^{-1}$ for a cyclic nonamer. Each level is labeled by its C_9 irreducible representation and its energy in cm^{-1} (e of eq 3 is set to zero). The strongly transition-allowed E_1 levels are placed at the B850 band maximum. At the upper left-hand corner is a simple diagram showing the arrangement of transition dipoles for a cyclic nonamer.

absorption, but the near in-plane (perpendicular to the C_9 axis) orientation of the BChl transition dipoles renders the A level essentially forbidden (carrying less than 1% of the absorption intensity of the B850 band according to the calculations of Sauer et al.⁶). For this reason, the E_1 level in Figure 1 is placed at the B850 band maximum. As discussed in refs 1 and 2, energy disorder splits the degeneracies of the E-type levels, couples energetically different levels, and provides forbidden levels with absorption strength by virtue of their mixing with the allowed

E_1 level. The tail absorption on the low-energy side of B850 is due to the A level (often referred to as B870). The high-energy tail absorption has recently been assigned to the E_2 level.² Hole-burning data show that at 4.2 K the inhomogeneous broadening of B870 (Γ_{inh}) is 120 cm^{-1} for high-quality samples, that the B870 absorption maximum lies 200 cm^{-1} to the red of the B850 maximum, and that B870 carries 3–5% of the total absorption intensity of the B850 band.¹⁰ These results were explained in terms of energy disorder.^{1,2,10} The situation where only the A, E_1 , and E_2 levels contribute to the B850 band also holds for *Rhodospirillum rubrum* for which the symmetry is C_8 (16 BChl molecules). On the basis of the results of Hu et al.,¹¹ the same would appear to be true for the B875 band of LH1 with its C_{16} symmetry (32 BChl molecules).

The high cyclic symmetry of the above nano-rings invites a group theoretical approach to the study of the effects of energy disorder since an arbitrary defect pattern can be written as a linear combination of the BDPs. By examining the effects from each BDP, one has a systematic approach to the question of whether energy disorder can account for spectroscopic data given a zero-order C_n -Hamiltonian.^{1,2} There are also strict selection rules governing the coupling of the zero-order exciton levels by the BDPs; see section 2. As shown here, however, the BDP approach is most useful for weak disorder. By weak disorder is meant that the disorder-induced coupling matrix elements between energetically different levels are comparable to or smaller than the zero-order level spacings. We show that the aforementioned complexes satisfy weak disorder. To do so one requires data that define the maximum (average) experimentally allowed disorder (MEAD). At this point we mention only that Wu et al.,² using the B850 profile shown in Figure 1 and $\Gamma_{\text{inh}} = 120 \text{ cm}^{-1}$, showed that the maximum average splitting of the degeneracy of the E_1 level is $\sim 60 \text{ cm}^{-1}$ and that absorption due to the E_3 and E_4 levels is not observed.²

The paper is organized as follows. Section 2 provides a review of the theory of ref 1 and definition of the exciton level participation number N which is a rough gauge of localization or extendedness (L–E). Section 3 presents the results of diagonal energy disorder calculations on the L–E (occupation number) patterns and N values for the C_9 system of Figure 1. (Similarities and differences between diagonal and off-diagonal disorder for weak and strong disorder as well as between C_9 and C_8 are discussed.) The results provide strong support for the suggestion by Wu et al.² that one need only consider a single BDP of e_1 ¹² symmetry to understand the effects of random disorder on the exciton levels that contribute to the B850 band. The section ends with results which show that consideration of energy disorder is important for interpretation of electric field (Stark) effects on this band. Conclusions are given in the last section along with additional remarks on utility of our symmetry-based approach.

2. Theoretical Background

We begin with a review of the main results from refs 1 and 2. In the presence of disorder the Hamiltonian for a C_n system is

$$H = H_0 + H_\lambda + H_\nu \quad (1)$$

where H_0 is the Hamiltonian in the absence of disorder with delocalized eigenfunctions

$$|j\rangle = n^{-1/2} \sum_{\alpha=0}^{n-1} B^{j\alpha} |\alpha\rangle \quad (2)$$

and energies

$$E_j = e + 2V \cos(2\pi j/n) \quad (3)$$

with $j = 0, 1, \dots, n-1$ labeling the delocalized exciton levels or irreducible representations (reps) of the C_n group. In eq 2, $B = \exp(i2\pi/n)$. The correspondence between j values and reps for $n = 9$ is as follows: $j = 0$ (A); $j = \{1, 8\}$ (E_1); $j = \{2, 7\}$ (E_2); $j = \{3, 6\}$ (E_3); and $j = \{4, 5\}$ (E_4). The two reps in each curly bracketed term are separately degenerate. An alternative and equivalent way of expressing the degenerate pairs is $\{1, -1\}$, $\{2, -2\}$, $\{3, -3\}$, and $\{4, -4\}$. For $n = 8$, another case of importance in photosynthesis, one has the following: $j = 0$ (A); $j = \{1, 7\}$ (E_1); $j = \{2, 6\}$ (E_2); $j = \{3, 5\}$; and $j = 4$ (B). In eq 3, e is the site excitation energy, V is the nearest neighbor coupling and α labels the ring site ($|\alpha\rangle$ is the localized site wave function). Returning to eq 1, H_λ and H_ν govern the diagonal and off-diagonal energy disorder, respectively. Starting with the usual expressions for H_λ and H_ν in the site representation and writing the site wave function as

$$|\alpha\rangle = n^{-1/2} \sum_j B^{j\alpha} |j\rangle \quad (4)$$

it follows that the couplings between delocalized levels r and s are given by^{1,2}

$$\langle r | H_\lambda | s \rangle = \frac{1}{n} \sum_{\alpha} \lambda_{\alpha} B^{(r-s)\alpha} \quad (5)$$

and

$$\langle r | H_\nu | s \rangle = \frac{1}{n} \sum_{\alpha} \nu_{\alpha} B^{(r-s)\alpha} (B^{-s} + B^r) \quad (6)$$

Here, λ_{α} is the diagonal energy defect at site α , and ν_{α} is the defect associated with coupling between sites α and $\alpha + 1$. It is at this point where one introduces the BDPs which transform like the reps of the C_n group. The BDPs are obtained using the projection operator technique.^{13,14} This technique would be familiar to those who, for example, have used it to generate the π molecular orbitals of benzene. The normalized C_9 coefficients of the BDPs for diagonal energy disorder are given in Table 1. To avoid confusion we use lower case Roman letters to label the reps for BDPs and upper case for the exciton levels. Inspection of Table 1 reveals that only the e_3 BDPs (with the obvious exception of the BDP carrying a symmetry) does not reduce the symmetry to C_1 . The e_3 BDPs reduce the symmetry to C_3 . Normalized C_8 coefficients are given in Table 2, from which one observes that the BDP of b symmetry reduces the C_8 symmetry to C_4 while BDPs of e_2 symmetry reduce C_8 to C_2 . The BDPs for off-diagonal disorder are precisely the same as those given in Tables 1 and 2 when the coefficients of the BDPs are rotated by $\pi/9$ and $\pi/8$, respectively, so as to be centered between neighboring sites. As mentioned earlier, any chosen energy defect pattern for the ring can be expressed as a superposition of BDPs since they form a complete set. Thus, one can examine the effects of each BDP on the ring exciton structure so as to determine which are of primary importance. Incorporation of the BDP in eq 5 leads to^{1,2}

$$\langle r | H_{\lambda}^{e_{j\pm}} | s \rangle = \frac{\lambda_{j\pm} N_{j\pm}}{n} \sum_{\alpha} \left[\cos\left(\frac{2\pi j\alpha}{n}\right) \pm \cos\left(\frac{2\pi j(\alpha-1)}{n}\right) \right] e^{i2\pi\alpha(r-s)/n} \quad (7)$$

TABLE 1: Normalized Coefficients of Basis Defect Patterns for C_9

| | site number | | | | | | | | |
|------------------|-------------|--------|--------|--------|--------|--------|--------|--------|--------|
| | 0 | 1 | 2 | 3 | 4 | 5 | 6 | 7 | 8 |
| a | 0.333 | 0.333 | 0.333 | 0.333 | 0.333 | 0.333 | 0.333 | 0.333 | 0.333 |
| e _{1,+} | 0.443 | 0.443 | 0.236 | -0.082 | -0.361 | -0.471 | -0.361 | -0.082 | 0.236 |
| e _{1,-} | 0.161 | -0.161 | -0.408 | -0.464 | -0.303 | 0 | 0.303 | 0.464 | 0.408 |
| e _{2,+} | 0.361 | 0.361 | -0.236 | -0.443 | 0.082 | 0.471 | 0.082 | -0.443 | -0.236 |
| e _{2,-} | 0.303 | -0.303 | -0.408 | 0.161 | 0.464 | 0 | -0.464 | -0.161 | 0.408 |
| e _{3,+} | 0.236 | 0.236 | -0.471 | 0.236 | 0.236 | -0.471 | 0.236 | 0.236 | -0.471 |
| e _{3,-} | 0.408 | -0.408 | 0 | 0.408 | -0.408 | 0 | 0.408 | -0.408 | 0 |
| e _{4,+} | 0.082 | 0.082 | -0.236 | 0.361 | -0.443 | 0.471 | -0.443 | 0.361 | -0.236 |
| e _{4,-} | 0.464 | -0.464 | 0.408 | -0.303 | 0.161 | 0 | -0.161 | 0.303 | -0.408 |

TABLE 2: Normalized Coefficients of Basis Defect Patterns for C_8

| | site number | | | | | | | |
|------------------|-------------|--------|--------|--------|--------|--------|--------|--------|
| | 0 | 1 | 2 | 3 | 4 | 5 | 6 | 7 |
| a | 0.354 | 0.354 | 0.354 | 0.354 | 0.354 | 0.354 | 0.354 | 0.354 |
| e _{1,+} | 0.462 | 0.462 | 0.191 | -0.191 | -0.462 | -0.462 | -0.191 | 0.191 |
| e _{1,-} | 0.191 | -0.191 | -0.462 | -0.462 | -0.191 | 0.191 | 0.462 | 0.462 |
| e _{2,+} | 0.354 | 0.354 | -0.354 | -0.354 | 0.354 | 0.354 | -0.354 | -0.354 |
| e _{2,-} | 0.354 | -0.354 | -0.354 | 0.354 | 0.354 | -0.354 | -0.354 | 0.354 |
| e _{3,+} | 0.191 | 0.191 | -0.462 | 0.462 | -0.191 | -0.191 | 0.462 | -0.462 |
| e _{3,-} | 0.462 | -0.462 | 0.191 | 0.191 | -0.462 | 0.462 | -0.191 | -0.191 |
| b | 0.354 | -0.354 | 0.354 | -0.354 | 0.354 | -0.354 | 0.354 | -0.354 |

for e-type BDPs. The \pm subscripts denote the partner BDPs for a given value of j . The set of square-bracketed terms with $\alpha = 0, 1, \dots, n-1$ define the defect pattern with $N_{j,\pm}$ being the normalization constant for the BDP (as defined in ref 1). The relationship between $\lambda_{j,\pm}$ and the λ value for the generator defect site (λ_g) used with the projection operator technique is $\lambda_{j,\pm}/N_{j,\pm} = \lambda_g$. In simpler terms, once the value of λ_g is set (without loss of generality one can associate λ_g with λ_0 for site “zero” of the ring), the values of the defect at all other sites are determined by symmetry as prescribed by Tables 1 and 2. For the totally symmetric (a) BDP, the square-bracketed term in eq 7 is replaced by unity for every site α . For n even, where one has a BDP of b symmetry, the square-bracketed term in eq 7 is replaced by $(-1)^\alpha$.

The matrix elements for off-diagonal disorder are given by¹

$$\langle r | H_{\nu}^{e_{j,\pm}} | s \rangle = \frac{\nu_{j,\pm} N_{j,\pm}}{n} \sum_{\alpha} \left[\cos\left(\frac{2\pi j \alpha}{n}\right) \pm \cos\left(\frac{2\pi j (\alpha-1)}{n}\right) \right] B^{(r-s)\alpha} [B^{-s} + B^r] \quad (8)$$

Coupling Selection Rules. The selection rule associated with the matrix elements of eqs 7 and 8 is^{1,2}

$$r - s = \pm j \quad (9)$$

with j defining the BDP which couple exciton levels r and s . The degeneracy of level E_r is removed, in first order, by a BDP with symmetry contained in the symmetric direct product $(E_r \times E_r)_+$. For C_9 with $r = 1-4$, the symmetries of the BDPs are, respectively, e_2 , e_4 , e_3 , and e_1 . For C_8 with $r = 1-3$, they are e_2 , b, and e_2 . These results also follow from eq 9.

The Participation Number N . The problem of localization of electrons or electronic excitations by energy disorder in infinite one- and higher dimensional structurally disordered solids is an old one¹⁵ but one of current interest (for reviews see refs 16–18. As it turns out, it is generally more difficult to determine and characterize extended (not perfectly localized at some site) states than a completely localized state.¹⁶ The brute force approach to the problem, where one imposes Gaussian randomness on site energies (H_λ) or nearest neighbor

site–site couplings (H_{ν}), poses an enormous computational problem, especially for macroscopic systems (thus, and as discussed in refs 16–18, scaling theories have been applied to the problem). In the course of studying the above problem the participation number N was introduced as a rough gauge for localization or extendedness. An eigenstate, $|\psi\rangle$, of the Hamiltonian for the disordered system can be expressed as

$$|\psi\rangle = \sum_{\alpha} c_{\alpha\psi} |\alpha\rangle \quad (10)$$

where $|\psi\rangle$ is the site wave function. The participation number N , which was recently used in the study of LH complexes of purple bacteria,^{19–21} is defined by

$$\frac{1}{N_{\psi}} = \sum_{\alpha} |c_{\alpha\psi}|^4 \quad (11)$$

In an aside to his review article,²² Thouless noted that $N_{\psi} = n$ for all states $|\psi\rangle$ of a perfect (no disorder) cyclic system, i.e., all states are completely delocalized. This result follows immediately from eqs 2, 10, and 11. He also concluded that, in the limit of very small random energy disorder, $N_{\psi} = 2n/3$ for all doubly degenerate levels (for nondegenerate levels such as A of C_9 or A and B of C_8 , $N_{\psi} = n$). Monshouwer et al.²¹ concluded that $N_{\psi} = 2n/3$ for degenerate levels *even* in the absence of disorder. This conclusion is incorrect since, in the absence of disorder, the Hamiltonian carries C_n symmetry, meaning that the wave functions must be of the Bloch type, as in eq 2. It is worthwhile to comment briefly on the derivation of the $N_{\psi} = 2n/3$ result which was not given by Thouless. The derivation follows once one notes that random disorder, no matter how small, destroys the C_n symmetry, meaning that one needs to abandon the Bloch wave functions of eq 2 and consider the sine- and cosine-type functions

$$|j_{\sin}\rangle = 2^{1/2} n^{-1/2} \sum_{\alpha} \sin(2\pi j \alpha / n) |\alpha\rangle \quad (12a)$$

and

$$|j_{\cos}\rangle = 2^{1/2} n^{-1/2} \sum_{\alpha} \cos(2\pi j\alpha/n) |\alpha\rangle \quad (12b)$$

in the limit where disorder approaches zero. Equations 12 and 11 would appear, with a first glance proof, to be consistent with the $N_{\Psi} = 2n/3$ result. However, closer inspection reveals that the proof breaks down whenever $j/n = 1/4$ (or an odd multiple of $1/4$), where j labels the exciton level and n is the order of the cyclic group. Thus, the $N_{\Psi} = 2n/3$ result is valid for n odd. For n even, one needs to be careful. For example, for $n = 6$ or 10 , the $N_{\Psi} = 2n/3$ result holds. It does not hold for $n = 8$ and the E_2 degenerate pair. It is not difficult to show that $N_{\Psi} = n/2 = 4$ for both components of E_2 of C_8 . For the case of C_{16} , $N_{\Psi} = n/2 = 8$ for the components of the E_4 exciton level.

3. Results and Discussion

As discussed in the Introduction, the C_9 arrangement of in-plane (perpendicular to the C_9 axis) transition dipoles shown in Figure 1 provides a good model for interpretation of spectroscopic data on the B850 absorption band of *Rps. acidophila*. The same is true for the corresponding band of *Rs. molischanum* and the B875 band of the LH1 complex for which C_9 is replaced by C_8 and C_{16} , respectively. For all three of these bands, only the A, E_1 , and E_2 exciton levels contribute, as indicated in Figure 1 for the B850 band of *Rps. acidophila*. Again, in the absence of energy disorder the E_2 level (also E_3 and E_4) is symmetry forbidden in absorption while the A level is rendered essentially forbidden because of the structure of the LH2 complex. In view of the calculations of Sauer et al.⁶ and Alden et al.,²³ we take the A level to be totally forbidden in the absence of disorder (their calculations indicate that the A level carries significantly less than 1% of the absorption cross section of the symmetry-allowed E_1 level). To understand what we mean by hidden correlation, we recall that when Gaussian randomness is imposed on the excitation energies or nearest neighbor couplings of the sites of infinite systems, one has a total absence of correlation. The same would be true for the nano-ring systems considered here, where the imposition of Gaussian randomness accounts for fluctuations in excitation energies or couplings as one moves from one ring to the next in the ensemble. On the other hand, the basis defect patterns defined in section 2 are perfectly correlated. That is, given a BDP and the value of the defect at one site, one automatically knows the values of the defects at all other sites. At first glance, one might think, therefore, that BDPs are of little use for understanding the effects of random energy disorder on nano-ring systems. This turns out not to be true for weak disorder as defined in section 1. That BDPs are potentially useful follows in this case when it is noted that any arbitrary defect pattern can be written as a linear combination of BDPs, that the matrix elements defined by eqs 7 and 8 are comparable to or small relative to the spacings between adjacent delocalized exciton levels and that disorder-induced coupling is governed by the selection rule $r - s = \pm j$ of eq 9. (Recall also that the first-order splitting of a degenerate exciton level r is determined by BDP of symmetry contained in $(E_r \times E_r)_{+}$.) Thus, one observes that e_1 BDPs could be of particular importance since they couple adjacent (most closely spaced) levels. The importance of e_1 BDPs for understanding the nature of the B850 absorption band has been pointed out by Wu et al.,² who emphasized that they couple both the forbidden A and E_2 levels with the strongly allowed E_1 level and that, for example, the absorption intensity of the A level and its displacement below the E_1 level are strongly influenced by BDPs of e_1 symmetry. The dominance of the e_1 BDP components of

random disorder patterns in determining the nature of the excitonic level structure underlying the B850 band is an example of what we mean by hidden correlation.

We proceed now to present the results of calculations which support the conclusions of Wu et al. and address the problem of the localization patterns for the A, E_1 , and E_2 levels associated with the B850 band of *Rps. acidophila*. Localization or extendedness for these levels was not considered by Wu et al. For the sake of brevity, we present results only for diagonal energy disorder although we comment on similarities and differences between diagonal and off-diagonal disorder.

We begin with results obtained with randomly generated diagonal defect patterns for the C_9 ring. For each random pattern the values of the site defects were uniformly scaled so as to yield results consistent with experimental results;¹⁰ namely, that the A level should carry ~5–10% of the total absorption intensity of the B850 band (denoted by $I(\%)$ in Table 3), that the energy spacing between the A and E_1 levels (ΔE in Table 3) should be ~200 cm^{-1} , and that the splitting of the degeneracy of the strongly allowed E_1 level (ΔE_1 in Table 3) should be no greater than ~60 cm^{-1} .² For the sake of brevity, any defect pattern that yields results consistent with these experimental results will be referred to as a MEAD (maximum experimentally allowed disorder) pattern. Each random pattern was then decomposed into its BDP components,¹ and their contributions to I , ΔE and ΔE_1 were analyzed. The conclusions to be drawn from the results given in Table 3 for a particular pattern are consistent with the results from other random defect patterns. They are also consistent with results obtained with diagonal disorder localized at a single site on the ring. We remind the reader that we are concerned with the weak disorder regime, one that is appropriate for the systems being considered. Line 19 of Table 3 gives the results for the random defect pattern with $I = 10.4\%$, $\Delta E = 208 \text{ cm}^{-1}$, and $\Delta E_1 = 34 \text{ cm}^{-1}$ (ΔE_2 , which is the splitting of the E_2 level degeneracy, is considered below). Lines 1 and 2 give the results for the $e_{1,+}$ and $e_{1,-}$ BDPs, respectively, while line 3 corresponds to the combination of $e_{1,+}$ and $e_{1,-}$. Comparison of the I and ΔE values of lines 1–3 with those of line 19 and the observation that $I = 0\%$ and $\Delta E \sim 150 \text{ cm}^{-1}$ (defect-free value) for every line in which the $e_{1,+}$ and $e_{1,-}$ contributions are excluded firmly establishes the importance of e_1 BDPs to the underlying level structure of the B850 band. Turning next to the ΔE_2 column, one can see that the degeneracy splitting of the E_2 level (77 cm^{-1} , line 19) is due almost entirely to e_4 BDPs, as expected from the selection rules given in section 2. With that in mind, the question arises as to why in lines 1–3 the ΔE_1 values are not close to zero since the e_2 BDPs which split the E_1 level in first order are excluded. The reason is that because the E levels are separably degenerate, a second-order mechanism for removal of degeneracy exists, one that involves coupling between levels subject to the selection rule of eq 9. That is, the e_1 BDPs in lines 1–3 couple the E_1 components with the nearby A and E_2 levels. This higher order effect is not important for the E_4 level since it is relatively far removed from the other levels. Not included in Table 3 are results for the percent intensity of the E_2 level. It is zero when the contributions from e_1 BDPs to the random pattern are excluded. This is expected since e_1 BDPs couple E_2 with the allowed E_1 level. Because the spacing between the E_2 and E_1 levels is larger than that between the A and E_1 levels, Figure 1, intensity borrowing by the E_2 level is less than that of the A level.

Localization or Extendedness. The above results indicate that e_1 BDPs, and to a lesser extent, e_2 BDPs are very important

TABLE 3: Calculated Results for a Random Diagonal Defect Pattern^a ($V = -320 \text{ cm}^{-1}$)

| line | $e_{1,+}$ | $e_{2,+}$ | $e_{3,+}$ | $e_{4,+}$ | $e_{1,-}$ | $e_{2,-}$ | $e_{3,-}$ | $e_{4,-}$ | I | ΔE | ΔE_1 | ΔE_2 |
|------|-----------|-----------|-----------|-----------|-----------|-----------|-----------|-----------|------|------------|--------------|--------------|
| 1 | X | | | | | | | | 6.8 | 184 | 27 | 0.1 |
| 2 | | | | | X | | | | 4.7 | 172 | 17 | 0.1 |
| 3 | X | | | | X | | | | 9.1 | 201 | 40 | 0.3 |
| 4 | | X | | | | X | | | 0.0 | 151 | 34 | 1.1 |
| 5 | | | X | | | | X | | 0.0 | 149 | 0.0 | 0.0 |
| 6 | | | | X | | | | X | 0.0 | 149 | 0.0 | 75 |
| 7 | X | X | | | X | X | | | 10.4 | 210 | 15 | 1.2 |
| 8 | X | | X | | X | | X | | 8.8 | 200 | 50 | 9.7 |
| 9 | X | | | X | X | | | X | 9.2 | 201 | 46 | 89 |
| 10 | | X | X | | | X | X | | 0.0 | 150 | 34 | 2.8 |
| 11 | | X | | X | | X | | X | 0.0 | 150 | 31 | 76 |
| 12 | | | X | X | | | X | X | 0.0 | 149 | 2.0 | 74 |
| 13 | X | X | X | | X | X | X | | 10.1 | 207 | 25 | 9.9 |
| 14 | X | X | | X | X | X | | X | 10.4 | 209 | 24 | 86 |
| 15 | X | | X | X | X | | X | X | 9.3 | 202 | 56 | 79 |
| 16 | | X | X | X | | X | X | X | 0.0 | 149 | 33 | 77 |
| 17 | X | X | X | X | | | | | 8.2 | 191 | 4.4 | 74 |
| 18 | | | | | X | X | X | X | 4.9 | 173 | 30 | 30 |
| 19 | X | X | X | X | X | X | X | X | 10.4 | 208 | 34 | 77 |

^a The disorders are 121, 148, 129, 137, 101, -157 , 10.4 , -113 , and 105 cm^{-1} at sites 0–8, respectively, generated randomly according to a Gaussian distribution centered at 0 with a standard deviation of 150 cm^{-1} . By using eq 16 of ref 1, the random defect pattern can be expressed as a linear combination of C_9 BDPs. The resulting λ_0 for a , $e_{1,+}$ through $e_{4,+}$, and $e_{1,-}$ through $e_{4,-}$ BDPs are 53.5, 91.2, -12.0 , 13.9, -12.0 , -25.5 , 19.5, 22.3, and -29.5 cm^{-1} , respectively. X's in a line indicate the BDP components of the random defect pattern being considered.

for understanding the underlying exciton level structure of the B850 band of *Rps. acidophila*. This is also the case for the B850 band of *Rs. molischianum* where the symmetry of the LH2 complex is C_8 and, most likely, also the B875 absorption band of the LH1 complex which carries C_{16} symmetry. We have performed a large number of calculations on the participation numbers (N) and localization–extendedness (L–E) patterns for C_9 and C_8 symmetry. By L–E pattern we mean the set $\{|c_{\alpha\psi}|^2\}_{\alpha=0}^{n-1}$ for the level $|\psi\rangle$, see eq 10. Thus, $|c_{\alpha\psi}|^2$ is the probability that the excitation resides on dimer α . The calculations included diagonal and off-diagonal random disorder and disorder associated with $e_{j,+}$ and $e_{j,-}$ BDPs (also the BDP of b symmetry for C_8).

Figure 2 shows the $e_{1,+}$ diagonal disorder L–E patterns for all exciton levels (A–E₄) of our C_9 system obtained for very weak disorder, $\lambda_0 = 1.8 \text{ cm}^{-1}$. λ_0 is the value of the energy defect at site “0”. Values of the defect at the other eight sites are readily obtained using Table 1. Each of the nine patterns shown are labeled by A or E _{j,l} or E _{j,h} , where l and h denote lower and higher energy components of the E _{j} levels whose 2-fold degeneracy is removed by disorder and $j = 1$ –4. At the top of each pattern are five-digit numbers which are the energies of the levels in the unit of cm^{-1} . (With reference to eq 3, e has been set equal to zero and $V = -320 \text{ cm}^{-1}$, vide supra.) To the immediate right of each energy value is the value of the participation number N . As predicted in section 2, $N = 6$ for all levels except the A level for which $N = 9$. These limiting N values are also obtained for the $e_{1,-}$, e_2 , and e_4 BDPs (e_3 BDPs yield different results since they leave the system with C_3 symmetry, although, for example, $N = 9$ for the A level). Furthermore, for very weak disorder, the L–E patterns from off-diagonal and diagonal disorder are the same. As can be seen from Figure 2, the patterns for levels E _{j} vary significantly with j and E _{j,l} and E _{j,h} patterns complement each other.

Figure 3 shows the L–E patterns obtained with $\lambda_0 = 140 \text{ cm}^{-1}$. This value of λ_0 for the $e_{1,+}$ BDP satisfies the MEAD condition. Note, for example, that $\Delta E = 220 \text{ cm}^{-1}$ and $\Delta E_1 = 56 \text{ cm}^{-1}$. The L–E patterns were found to change smoothly as λ_0 was increased from 1.8 cm^{-1} to higher values.²⁴ Comparison of Figures 2 and 3 reveals how the A level has

undergone a single “clump” localization for $\lambda_0 = 140 \text{ cm}^{-1}$ with $N = 4.9$. Since the B850 sites are dimers, the number of BChl molecules which contribute significantly is ~ 10 .²⁵ One observes also that the E_{4,l} level is more extended at $\lambda_0 = 140 \text{ cm}^{-1}$ than at $\lambda_0 = 1.8 \text{ cm}^{-1}$, in contrast with the E_{4,h} level. Thus, the well-known adage that increasing diagonal energy disorder leads to greater localization for all levels does *not* generally pertain to the systems considered here. The increase in N for E_{4,l} from 6.0 to 7.5 is compensated by the decrease in N for E_{4,h} to 4.4. We note that L–E patterns of the $e_{1,-}$ BDP are similar to those of the $e_{1,+}$ BDP for C_9 and weak disorder. Significant differences occur for strong disorder.²⁴ (For C_8 , $e_{j,+}$ and $e_{j,-}$ BDPs yield identical results since their BDPs are related by a $\pi/4$ or $\pi/2$ rotation, see Table 2.)

We investigated the effects of adding e_2 BDPs to e_1 BDPs since e_2 BDPs split the degeneracy of the E₁ level in first order. The L–E patterns have been obtained with $\lambda_0(e_{1,+}) = 140 \text{ cm}^{-1}$ (the value used in Figure 3) and a very small value for $\lambda_0(e_{2,-})$ of -4.1 cm^{-1} (results not shown). Comparison with Figure 3 reveals that this $e_{2,-}$ disorder has essentially no effect on the L–E patterns (as expected, the energies of the E_{1,h} and E_{1,l} levels are slightly perturbed). This is also the case when $e_{2,+}$ is added rather than $e_{2,-}$ and when $e_{1,+}$ is replaced by $e_{1,-}$. Figure 4 gives the results for $\lambda_0(e_{1,+}) = 140 \text{ cm}^{-1}$ and $\lambda_0(e_{2,-}) = -50 \text{ cm}^{-1}$, a MEAD value. Comparison of this figure with Figure 3 ($\lambda_0(e_{1,+}) = 140 \text{ cm}^{-1}$) shows that the A level is hardly affected by the $e_{2,-}$ defect pattern, as expected. Interestingly, its effect on E_{1,l} and E_{1,h}, although greater than its effect on the A level, is not profound even though the $e_{2,-}$ BDP splits the E₁ degeneracy in first order; the E_{1,l} and E_{1,h} energies are shifted by only about -10 cm^{-1} , and their participation numbers change by -0.4 and $+0.5$, respectively. The weak effect on the E₁ levels is, to a considerable extent, a consequence of their second-order couplings with the A and E₂ levels via the $e_{1,+}$ BDP. Such couplings are likely mainly responsible for the significant increase in the extendedness of the E_{2,l} and E_{2,h} levels with the addition of the $e_{2,-}$ defect pattern.

Before presenting L–E patterns for random diagonal energy disorder, it is instructive to examine the patterns for e_4 BDPs. Results are given in Figure 5 for $\lambda_0(e_{4,+}) = 12 \text{ cm}^{-1}$, a MEAD

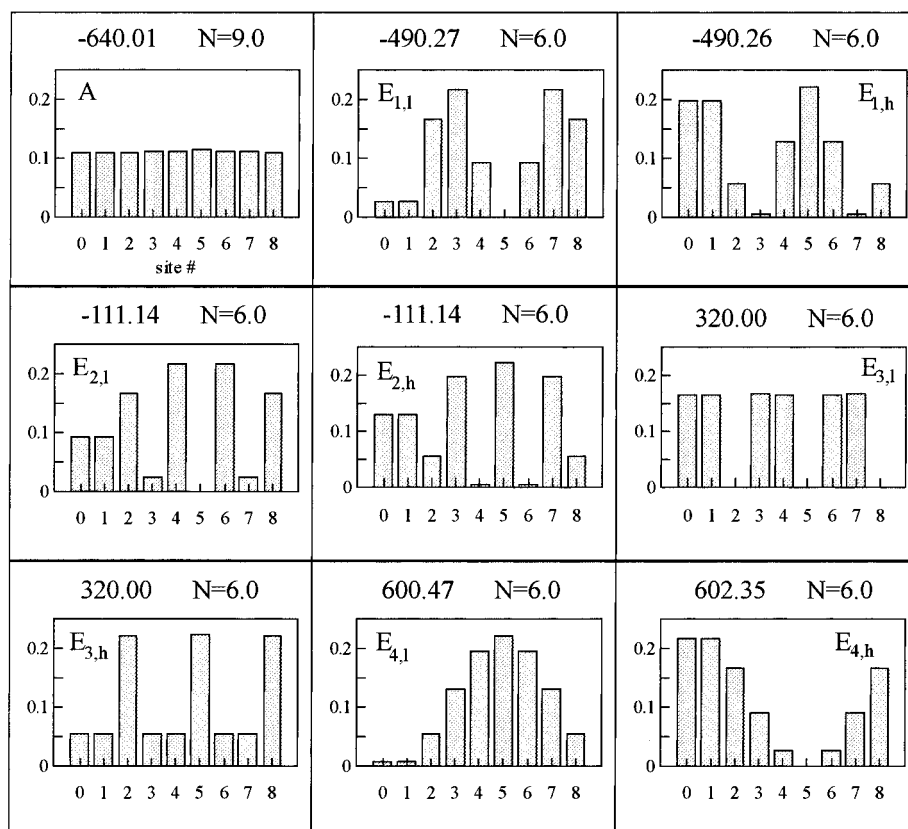


Figure 2. Localization–extendedness (L–E) patterns for the exciton levels of a C_9 ring in the presence of very weak $e_{1,+}$ diagonal energy disorder ($\lambda_0 = 1.8 \text{ cm}^{-1}$; $V = -320 \text{ cm}^{-1}$). Since the nine chromophores labeled by the integers 0 to 8 are arranged on the ring, sites 0 and 8 are nearest neighbors. Included at the top of each pattern is the energy of the level in cm^{-1} and the corresponding participation number N . See text for further explanation.

value which splits the degeneracy of the E_2 level by 69 cm^{-1} in first order. The major point is that the L–E patterns and participation numbers are very similar to those shown in Figure 2 for very weak disorder ($e_{1,+}$) which splits the degeneracy of the E_4 level by only 2 cm^{-1} . That much stronger e_4 disorder has only a weak effect is a consequence of it coupling only the A and E_4 levels which are far removed from each other, Figure 1. The L–E patterns for $E_{2,l}$ and $E_{2,h}$ of Figure 5 are essentially set by the sine- and cosine-type wave functions of eq 12.

L–E patterns for *random* diagonal disorder (MEAD) are shown in Figure 6. Uniform reduction of the site defects by a factor of 10 yielded L–E patterns similar to those of Figure 2 (results not shown). Comparison of Figures 6 and 3 ($\lambda_0(e_{1,+}) = 140 \text{ cm}^{-1}$) is of particular interest since both correspond to MEAD. Importantly, the patterns for the A and E_1 levels, which are of primary interest, are similar (confirmed for other random disorder patterns). This is also the case for the E_2 and E_4 levels.

To summarize, we have demonstrated that the effects of random diagonal energy disorder on level structure underlying the B850 band of *Rps. acidophila* can be investigated using a single e_1 -type BDP (hidden correlation effect). This affords a substantial simplification for computational studies along with a deeper understanding of the physics involved. Now one need only place a Gaussian distribution on $\lambda_0(e_{1,+})$ or $\lambda_0(e_{1,-})^2$ to explore localization–extendedness, exciton level absorption intensities, and other spectroscopic properties of individual complexes in an ensemble. In ref 2, Wu et al. used a half-Gaussian distribution for $\lambda_0(e_{1,+})$ with a width of 140 cm^{-1} to simulate B870 absorption spectrum. The width of 115 cm^{-1} for the profile and its ΔE value of $\sim 200 \text{ cm}^{-1}$ were in good agreement with the low-temperature values determined by zero-phonon hole action spectroscopy.¹⁰ The hidden correlation

effect proposed in this paper justifies their use of $e_{1,+}$ BDP alone in the simulation.

C_8 and C_{16} Ring Systems. Diagonal energy disorder calculations were also performed on the C_8 B850 ring of BChl molecules of *Rs. molischianum*. Briefly, it was also found that the effects of random disorder on the exciton levels contributing to its B850 band are well modeled using an e_1 -type BDP, cf. Table 2. Extensive calculations have not yet been performed on the C_{16} ring of LH1 although preliminary results indicate that e_1 -type BDPs can also be used for its B875 band.

Diagonal vs Off-Diagonal Random Energy Disorder. One expects differences in the L–E patterns from these two types of random disorder since the equivalent of a single-site diagonal defect for off-diagonal disorder involves two nearest neighbor sites. An interesting question is how strong the random disorder needs to be in order for the L–E patterns from the two types of disorder to be significant? We have performed some calculations which speak to this question. In the limit of very weak random disorder, the diagonal and off-diagonal L–E patterns for the exciton levels of our C_9 system were found to be identical. In the limit of very strong diagonal disorder, $N = 1$ for all levels. In sharp contrast, the N values from off-diagonal random disorder are in the range of ~ 2 – 3 . In other words, no matter how strong the off-diagonal random disorder, no level becomes completely localized. Other calculations showed that significant differences between the L–E patterns from the two types of disorder onset in the weak disorder regime, weaker than the MEAD condition defined earlier. Calculations were also performed for “single-site” disorder. We mention only that in the limit of very strong single-site diagonal disorder, one level is totally localized ($N = 1$) while $N = 2n/3 = 6$ for all other levels. These findings are understandable when one

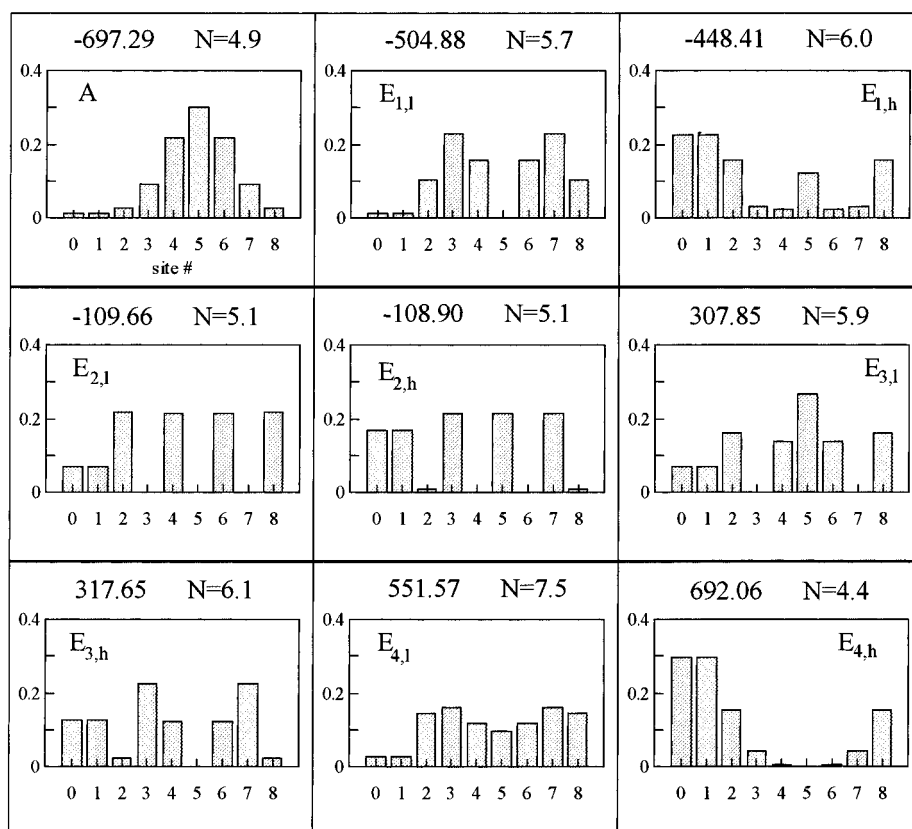


Figure 3. Localization-extendedness (L-E) patterns obtained with $\lambda_0(e_{1,+}) = 140 \text{ cm}^{-1}$; see Figure 2 caption.

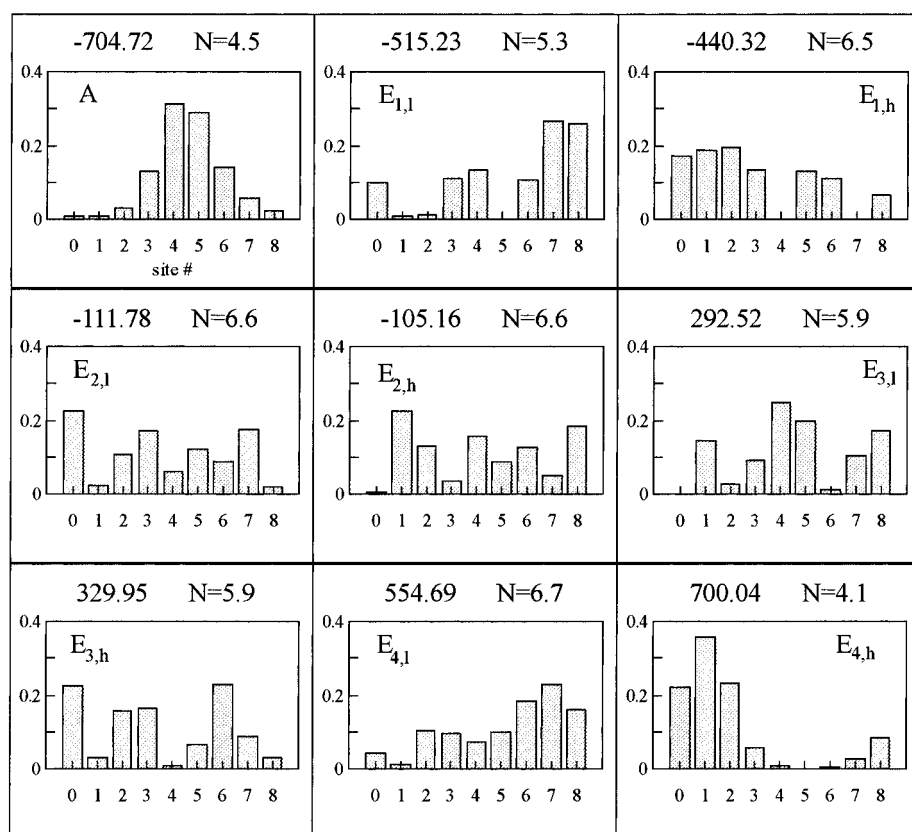


Figure 4. Localization-extendedness (L-E) patterns obtained with $\lambda_0(e_{1,+}) = 140 \text{ cm}^{-1}$ and $\lambda_0(e_{2,-}) = -50 \text{ cm}^{-1}$; see Figure 2 caption.

recognizes that in this limit, one has essentially a linear *J*-aggregate with $n = 9 - 1 = 8$. Indeed, the L-E patterns for such a *J*-aggregate were found to be very similar to those of the C_9 ring.

Energy Disorder and the Stark Effect. Recently, we reported Stark hole-burning results on the A (B870) exciton level of the B850 ring for *Rps. acidophila*, *Rs. molischianum*, and *Rhodobacter sphaeroides*.²⁶ The quantity of interest which

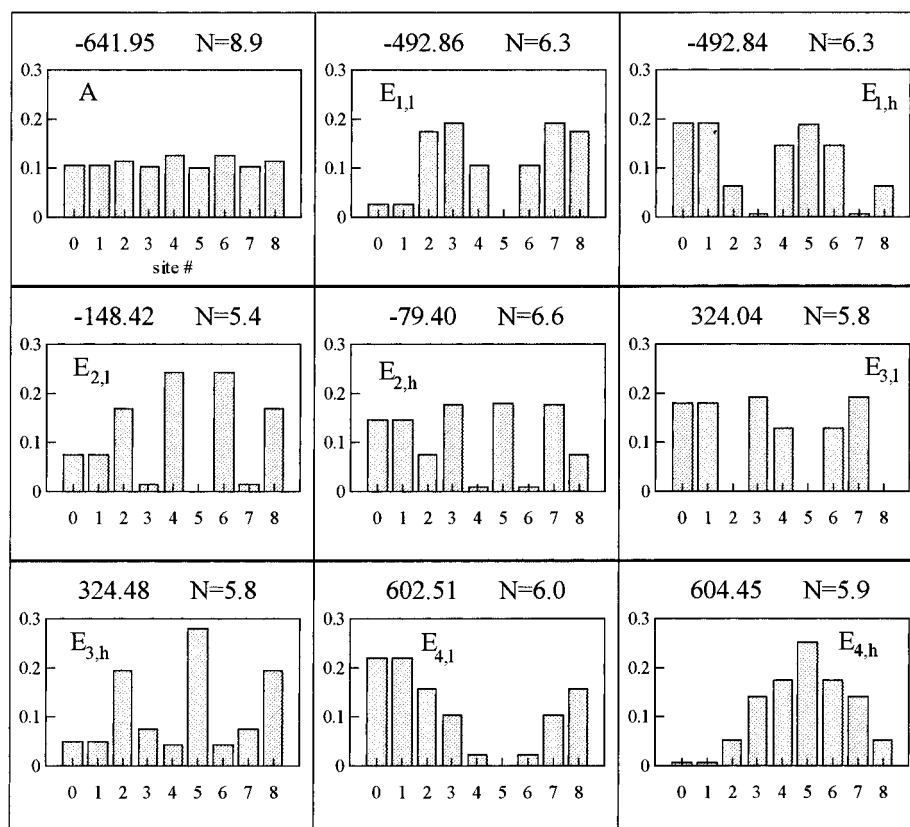


Figure 5. Localization-extendedness (L-E) patterns obtained with $\lambda_0(e_{4,+}) = 12 \text{ cm}^{-1}$; see Figure 2 caption.

is determined in such experiments is $|\Delta\mu| \equiv \Delta\mu$, the permanent dipole moment change between the ground electronic state and the A level. In that reference it was pointed out that $\Delta\mu$ for the A level is similar for all three species ($f\Delta\mu \sim 1.2 \text{ D}$, where f is the local field correction) and that this value is a factor of 3 smaller than the values determined by classical Stark modulation spectroscopy (SMS) on the *entire* B850 absorption band.²⁷ The analysis of the data in ref 27 assumed that all levels which contribute to the B850 band carry the same $\Delta\mu$ value and vector sense in the single complex (the effects of energy disorder were not considered). We present one line of argument for the just-mentioned assumptions of ref 27 requiring scrutiny. As reviewed in ref 28, earlier Stark optical experiments on the BChl molecule indicate that $\Delta\mu$ is quite close to being parallel to the in-plane y-axis of the molecule. INDO quantum chemical calculations that, for all intent and purposes, $\Delta\mu$ of the BChl molecule is parallel to the y-axis.²⁹ Given the structure of the LH2 complex, one can view dipole vectors on the ring shown in Figure 1 as the in-the-membrane-plane (i.p.) molecular contributions to the dipole moment change of individual sites. Independent of the way the symmetry-related i.p. dipoles of sites are oriented on the circle, $\Delta\mu_{i,p} = 0$ for *all exciton levels of the entire ring in the absence of energy disorder*. This state of affairs changes significantly when energy disorder is introduced as will be discussed in detail elsewhere.³⁰ Here we present only $\Delta\mu_{i,p}$ results for $e_{1,+}$ disorder for $\lambda_0 = 1.8$ (very weak disorder), 70, and 140 cm^{-1} (MEAD), Figure 7.

A value of 1.0 (arbitrary unit) for $\Delta\mu_{i,p}$ corresponds to the value of the dipole moment change for the single site (dimer). Except for the E_4 levels, $\Delta\mu_{i,p}$ is close to zero for very weak disorder. That the E_4 levels carry a significant dipole moment change is consistent with their single-clump L-E patterns shown

in Figure 2. The $E_{4,l}$ and $E_{4,h}$ patterns become more and less extended, respectively, as λ_0 increases, see Figure 3. This explains the opposite dependence of their $\Delta\mu_{i,p}$ value on λ_0 seen in Figure 7. Of particular relevance to the B850 band are the A- E_2 levels. Figure 7 reveals that, even for MEAD, $\Delta\mu_{i,p} < 1.0$ for all levels and that the largest $\Delta\mu_{i,p}$ values occur at the bottom (A level) and top of the exciton band. As one proceeds toward the middle of the band, $\Delta\mu_{i,p}$ decreases as a result of the E_2 and E_3 level L-E patterns being more equally distributed around the ring, see Figure 3. These general features were shown to hold for random diagonal disorder. The $E_{1,l}$ and $E_{1,h}$ levels, which are the main contributors to the B850 band, carry comparable absorption intensities. Figure 7 shows, however, that their $\Delta\mu_{i,p}$ values differ by about a factor of 2. Just as important, is that their $\Delta\mu_{i,p}$ vectors are not parallel, making instead an angle of 180° . The angles $\Delta\mu_{i,p}(E_{1,l})$ and $\Delta\mu_{i,p}(E_{1,h})$ make with $\Delta\mu_{i,p}(A)$ are 0 and 180° , respectively. In future work we plan to determine whether energy disorder can explain the aforementioned discrepancy between the $\Delta\mu$ values determined by SMS and Stark hole burning. In so doing, one needs to take into account the out-of-the-membrane-plane component of $\Delta\mu$.

Finally, we point out that in using e_1 BDPs to model the effects of energy disorder, one must take into account a distribution of $\lambda_0(e_1)$ values.² Concerning high-resolution hole-burning experiments, *single* complexes are not probed. Rather, one interrogates a subset of complexes whose zero-phonon absorption lines are degenerate. Members of this subset can have protein conformations which, from the perspective of glasslike disorder, differ significantly. Thus in hole burning, a distribution of λ_0 values must still be reckoned with. This reasoning is consistent with the observation in ref 26 that $\Delta\mu$

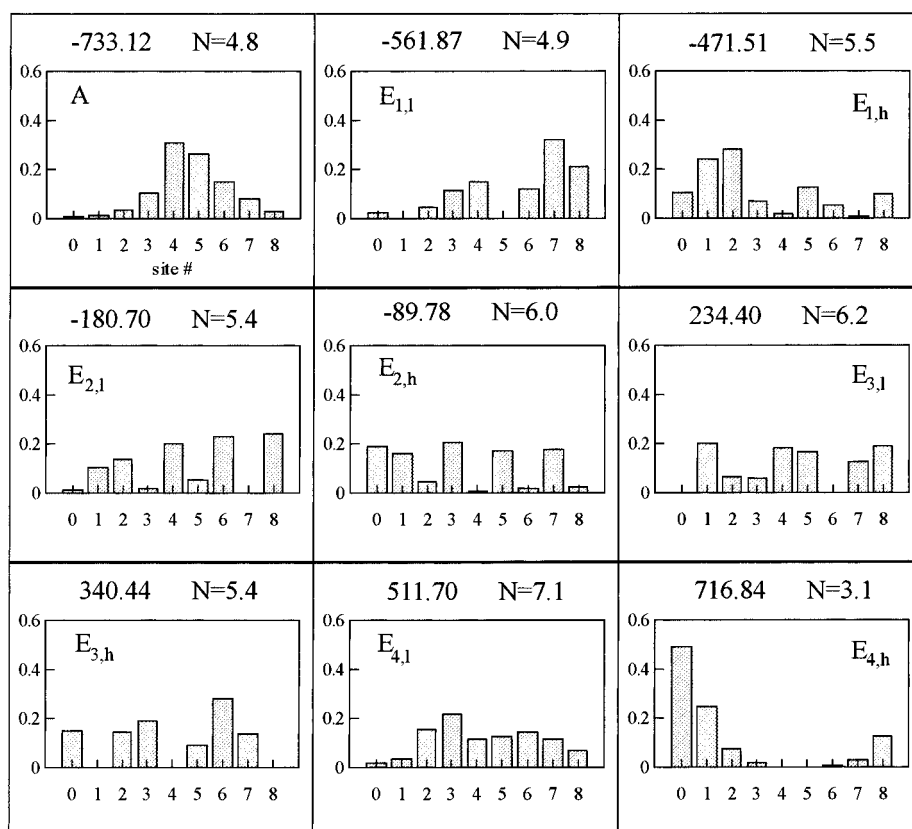


Figure 6. Localization-extendedness (L-E) patterns obtained with a random diagonal disorder for the C_9 ring. The disorders are 329, 83.5, -18.1, 6.53, -253, -143, -71.0, -102, -65.8 cm^{-1} at sites 0-8, respectively. These values were generated randomly for a Gaussian distribution centered at 0 and with a standard deviation of 150 cm^{-1} . By using eq 16 of ref 1, the random defect pattern can be expressed as a linear combination of C_9 BDP. The resulting λ_0 values for a, $e_{1,+}$ through $e_{4,+}$, and $e_{1,-}$ through $e_{4,-}$ BDPs are -26.0, 157, 42.3, 24.8, 7.76, 4.01, -3.67, 89.3, and 33.1 cm^{-1} , respectively.

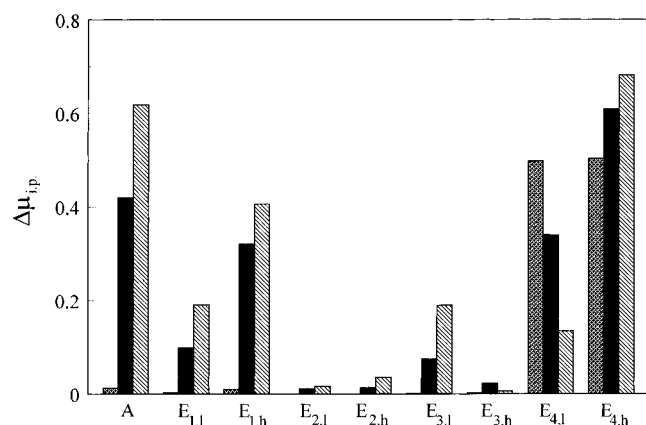


Figure 7. The in-plane permanent dipole moment change ($\Delta\mu_{i,p}$) for all exciton levels of C_9 in the presence of $e_{1,+}$ diagonal energy disorder. For each level, λ_0 is 1.8, 70, and 140 cm^{-1} from left to right, respectively. $\Delta\mu_{i,p} = 1.0$ (arbitrary units) for a single site. For $\lambda_0(e_{1,+}) = 1.8 \text{ cm}^{-1}$, $\Delta\mu_{i,p}$ for all levels is ~ 0 except for $E_{4,l}$ and $E_{4,h}$; see text.

for the A level (B870) of the B850 manifold varied only slightly as the burn frequency was tuned across the inhomogeneously broadened absorption profile of B870.

4. Concluding Remarks

In this paper we have explored further the usefulness of basis energy defect patterns for analysis of the effects of static energy disorder on the excitonic level structure of C_n LH complexes of purple bacteria. On the basis of a comparison of the localization-extendedness (L-E) or occupation number patterns

as well as participation numbers (N) stemming from random disorder and from individual BDPs, we conclude that the effects of diagonal or off-diagonal disorder at low temperatures on the A, E_1 , and E_2 levels which contribute to the B850 absorption band can be understood using a single e_1 BDP, the hidden correlation effect. (This is also likely the case for the B875 band of LH1.) The hidden correlation effect is a consequence of the structural details of the complexes and the fact that the complexes fall in the weak disorder regime where the zero-order levels spacings are greater than or comparable to the disorder-induced couplings between energetically different levels. The above conclusion is likely to hold at room temperature since the temperature dependencies of the B800 and B850 bands of the LH2 complex and the B875 band of LH1 indicate that their inhomogeneous broadenings are weakly dependent on temperature²¹ (see Monshouwer et al.²¹ for additional arguments).

The ability to use a single e_1 BDP greatly simplifies computational studies of the effects of random static disorder on the spectroscopic and photophysical properties of the B850 and B875 bands since one need only consider a single Gaussian distribution for say $\lambda_0(e_{1,+})$, in the case of diagonal disorder. (λ_0 is the value of the defect at site zero, the generator site.) This is the procedure used in ref 2 where the focus was on understanding the displacement of the A level (B870) below the B850 absorption maximum as well as the B870 absorption intensity. In addition to computational simplicity, one gains valuable insight on which disorder-induced couplings are most important. It should be noted that the usefulness of BDPs becomes limited as one moves into the strong disorder regime

or when n becomes too large. We see no reason why our symmetry-based approach would not be useful for reasonably short linear arrays in the weak disorder regime.

The C_9 L–E patterns of Figures 2–6 appear to be the most detailed yet reported for a C_n system. An interesting observation for the weak disorder regime is that the patterns for the split components of degenerate exciton levels E_j are already essentially set in the limit of *very weak* disorder (compare Figures 2 and 3). An explanation for this based on eqs 12a,b was given. Certain confusions over the exciton level participation numbers N for C_n systems in the limit of infinitesimally small random disorder were clarified. For n odd, $N(A) = n$ and $N = 2n/3$ for the two components of all degenerate levels. For n even, $N(A) = N(B) = n$ but $N(E_{j,l}, E_{j,h}) = n/2$ when $j/n = 1/4$ (or an odd multiple of $1/4$). For all other degenerate levels the $2n/3$ result still holds.

Although the results presented are for diagonal energy disorder and the C_9 B850 ring of *Rps. acidophila*, calculations were also performed for off-diagonal energy disorder for random and BDP defect patterns. For magnitudes of disorder which lie well within the weak disorder regime (vide supra), the L–E patterns and participation numbers were found to be similar for diagonal and off-diagonal disorder. As the strong disorder limit is approached, some significant differences occur, and as one moves well into the strong disorder regime, similarities between the two types of disorder essentially disappear, see section 3. The question of whether for the LH complexes one has to worry about off-diagonal disorder is a difficult one. We suggest, however, that it is relatively unimportant. Our reasoning is based on the fact that, at low temperatures, the inhomogeneous broadenings (slightly greater than 100 cm^{-1}) of the B850 and B875 bands are a factor of 2–3 times smaller than those of *isolated* “guest” molecules in glasses and polymers; this, despite the fact that in the LH complexes one has strong nearest neighbor BChl–BChl couplings. Perhaps more convincing is that the inhomogeneous broadening of the B800 absorption band of the LH2 complex is identical with that of the B850 band.⁹ The 9 and 8 BChls of the B800 rings of *Rps. acidophila* and *Rs. molischianum* are weakly coupled with V approximately -25 cm^{-1} ,^{6,31} compared to the nearest neighbor dimer–dimer couplings of approximately -300 cm^{-1} for the B850 ring. Thus, we think it most likely that the energy disorder which is of primary importance for the B850 and B875 rings is of the diagonal type caused by small glasslike fluctuations in the structure of the α,β polypeptide pair as one moves around the ring and between single rings of the ensemble of complexes which are studied.

It was shown that the L–E patterns and their associated permanent dipole moments are important for interpretation of electric field effects on the B850 absorption band. Such patterns as well as the corresponding wave functions are required for calculation of phonon-induced interexciton-level relaxation rates,^{32–34} a firm understanding of exciton delocalization or extendedness, and superradiance from single or ensembles of complexes.^{21,35} The superradiance enhancement is defined as the radiative dipole strength of the exciton level divided by that of the isolated chromophore. Monshouwer et al.²¹ measured an enhancement of 2.8 for the A (B870) level of an ensemble of LH2 complexes at 4.2 K. Since this level is essentially forbidden for perfect C_n symmetry, the superradiance is the result of energy disorder which also leads to clump localization of the A level. One can calculate the enhancement from the percentage of the total absorption of the B850 ring carried by B870. On the basis of the results of calculations presented here

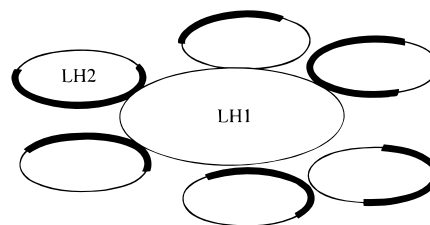


Figure 8. LH2 complexes surrounding the LH1 complex which encircles the reaction center. The broad dark lines of the LH2 rings are meant to indicate the “clump” localization of the A (B870) exciton level of LH2. The actual arrangement of LH2 complexes is not known.

and in ref 2, we estimate an average percentage of ~ 10 . For 18 BChl molecules one has, therefore, an average enhancement of ~ 2 . The reader is referred to ref 35 for a detailed discussion on the temperature dependence of superradiance.

Finally, we suggest that the clump L–E patterns of the B870 level might be important for understanding the LH2 \rightarrow LH1 energy transfer process, especially at low temperatures. This can be seen from Figure 8 which shows an arrangement of LH2 complexes around the LH1 complex. The broad dark lines of the former are meant to indicate the localization regions for the B870 level. The distribution of distances between these regions and the BChl molecules of the LH1 ring could lead to dispersive kinetics for the above transfer process. Such kinetics have recently been reported.³⁶

Acknowledgment. Research at the Ames Laboratory was supported by the Division of Chemical Sciences, Office of Basic Energy Sciences, U.S. Department of Energy. Ames Laboratory is operated for USDOE by Iowa State University under Contract W-7405-Eng-82. We thank R. Monshouwer and R. van Grondelle of the Vrije Universiteit of The Netherlands and S. Mukamel of the University of Rochester for preprints of their works prior to publication and J. Fajer and M. Newton of Brookhaven National Laboratory for providing us with their calculated permanent dipole moments for the BChl molecules of the FMO complex. The authors also thank S. Mukamel for useful discussions concerning various mechanisms, static disorder, and dynamics which lead to localization effects in nanosystems and Costas Soukalis of Iowa State University for enlightening us on recent advances in the understanding of disorder-induced localization effects in non-organic systems.

References and Notes

- (1) Wu, H.-M.; Small, G. J. *Chem. Phys.* **1997**, *218*, 225.
- (2) Wu, H.-M.; Ratsep, M.; Lee, I.-J.; Cogdell, R. J.; Small, G. J. *J. Phys. Chem. B* **1997**, *101*, 7654.
- (3) Koepke, J.; Hu, X.; Muenke, C.; Schulten, K.; Michel, H. *Structure* **1996**, *4*, 581.
- (4) Freer, A. A.; Prince, S. M.; Sauer, K.; Papiz, M. Z.; Hawthornthwaite-Lawless, A. M.; McDermott, G.; Cogdell, R. J.; Isaacs, N. W. *Structure* **1996**, *4*, 449.
- (5) Karrasch, S.; Bullough, P. A.; Ghosh, R. *EMBO J.* **1995**, *14*, 631.
- (6) Sauer, K.; Cogdell, R. J.; Prince, S. M.; Freer, A. A.; Isaacs, N. W.; Scheer, H. *Photochem. Photobiol.* **1996**, *64*, 564.
- (7) There are nine weakly coupled BChl molecules at the cytoplasmic side of the membrane which give rise to an absorption band at 800 nm, the B800 band. It is only the B850 band that is of interest here.
- (8) It is the $S_1(Q_y) \leftarrow S_0 \pi\pi^*$ transition of the BChl molecule that is involved.
- (9) Wu, H.-M.; Ratsep, M.; Jankowiak, R.; Cogdell, R. J.; Small, G. J. *J. Phys. Chem. B* **1997**, *101*, 7641.
- (10) Wu, H.-M.; Reddy, N. R. S.; Small, G. J. *J. Phys. Chem. B* **1997**, *101*, 651.
- (11) Hu, X.; Ritz, T.; Damjanovic, A.; Schulten, K. *J. Phys. Chem. B* **1997**, *101*, 3854.
- (12) To avoid confusion with exciton levels we use lower case letters for BDP symmetries.

- (13) Tinkham, M. *Group Theory and Quantum Mechanics*; McGraw-Hill: New York, 1964.
- (14) Hochstrasser, R. M. *Molecular Aspects of Symmetry*; W. A. Benjamin Inc.: New York, 1966.
- (15) Anderson, P. W. *Phys. Rev.* **1958**, *109*, 1492.
- (16) Lee, P. A.; Ramakrishnan, T. V. *Rev. Mod. Phys.* **1985**, *57*, 287.
- (17) Kramer, B.; MacKinnon, A. *Rep. Prog. Phys.* **1993**, *56*, 1469.
- (18) Skinner, J. L. *J. Phys. Chem.* **1994**, *98*, 2503.
- (19) Jimenez, R.; Dikshit, S. N.; Bradforth, S. E.; Fleming, G. R. *J. Phys. Chem.* **1996**, *100*, 6825.
- (20) Kühn, O.; Sundström, V. *J. Phys. Chem. B* **1997**, *101*, 3432.
- (21) Monshouwer, R.; Abrahamsson, M.; van Mourik, F.; van Grondelle, R. *J. Phys. Chem. B* **1997**, *101*, 7241.
- (22) Thouless, D. J. *Phys. Rep.* **1974**, *13*, 93.
- (23) Alden, R. G.; Johnson, E.; Nagarajan, V.; Parson, W. W.; Law, C. J.; Cogdell, R. G. *J. Phys. Chem. B* **1997**, *101*, 4667.
- (24) Interestingly, when λ_0 of $e_{1,+}$ becomes very large (infinite disorder limit), $N = 1$ for one level and $N = 2$ for all others. For the $e_{1,-}$ BDP, $N = 1$ for all levels. An explanation for this difference can be found in Table 1. It is found that for $e_{1,+}$ there are pairs of sites that have the same defect value, whereas for $e_{1,-}$, all sites have different defect values (the same behavior exists for the e_2 and e_4 BDP). For random disorder, the probability that two or more sites have the same defect value is vanishingly small. Thus, for diagonal energy disorder, $N = 1$ for all levels in the infinite disorder limit. For off-diagonal disorder this is not the case; see text.
- (25) We remind the reader that our calculations are tailored to low-temperature data.
- (26) Ratsep, M.; Wu, H.-M.; Hayes, J.; Small, G. J. *Spectrochim Acta A*, in press.
- (27) Beekman, L. M. P.; Frese, R. N.; Fowler, G. J. S.; Picorel, R.; Cogdell, R. J.; van Stokkum, I. H. M.; Hunter, C. N.; van Grondelle, R. *J. Phys. Chem. B* **1997**, *101*, 7293.
- (28) Lockhart, D. J.; Boxer, S. G. *Proc. Natl. Acad. Sci. U.S.A.* **1988**, *85*, 107.
- (29) Gudowska-Nowak, E.; Newton, M. D.; Fajer, J. *J. Phys. Chem.* **1990**, *94*, 5795.
- (30) Ratsep, M.; Wu, H.-M.; Hayes, J.; Small, G. J., submitted.
- (31) The B800 L-E patterns for $V = -25 \text{ cm}^{-1}$ were calculated for the random defect pattern of Figure 8. The A, E_1 , and E_4 levels were found to be essentially localized at a single site.
- (32) Davydov, A. S. *Theory of Molecular Excitons*; Plenum Press: New York, 1971.
- (33) Hochstrasser, R. M.; Prasad, P. N. In *Excited States*; Lim, E. C., Ed.; Academic Press: New York, 1974; Vol. 1, p 79.
- (34) Johnson, C. K.; Small, G. J. In *Excited States*; Lim, E. C., Ed.; Academic Press: New York, 1982; Vol. 6, p 97.
- (35) Meier, T.; Chernyak, V.; Mukamel, S. *J. Phys. Chem. B* **1997**, *101*, 7332.
- (36) Nagarajan, V.; Alden, R. J.; Williams, J. C.; Parson, W. W. *Proc. Natl. Acad. Sci. U.S.A.* **1996**, *93*, 13774.